Engineering Structures 46 (2013) 737–747

Contents lists available at SciVerse ScienceDirect

Engineering Structures

journal homepage: www.elsevier.com/locate/engstruct

# Seismic testing of steel braced frames with aluminum shear yielding dampers

Durgesh C. Rai *, Praveen K. Annam, Tripti Pradhan

*Dept. of Civil Engineering, Indian Institute of Technology Kanpur, Kanpur 208 016, India*

ARTICLE INFO

*Article history:*
Received 23 May 2011
Revised 20 August 2012
Accepted 29 August 2012
Available online 6 October 2012

*Keywords:*
Seismic
Energy dissipation
Aluminum
Hysteretic
Shear link
Braced frames
Shake table testing
Scaled models

ABSTRACT

A shake table study of single-bay two-storey model of conventional ordinary concentric braced frame (OCBF) and aluminum shear-link enabled braced frame (SLBF) was conducted to evaluate the performance of shear-link as energy dissipation device. The 1:12 reduced scale models were subjected to Taft ground motion of increasing peak ground accelerations, representing seismic loads of increasing severity. Similitude laws for adequate modeling of dynamic behavior of the reduced models were satisfied and time, frequency and acceleration values were scaled. The test indicated that SLBF frame attracted about 41–64% less base shear compared to OCBF for varying PGA levels of the ground motions. Similar trend was noticed for overturning moments and floor acceleration as well. However, the first storey floor drifts for the SLBF were always greater than the OCBF. Significant amount of energy was absorbed by aluminum shear-links leading to satisfactory response up to the scaled PGA of 1.7*g* of the Taft motion, while the OCBF frame could not survive the scaled PGA of 0.8*g*. These proof-of-concept tests also helped validate the design methodology developed for proportioning aluminum shear-link enabled steel frames.



## 1. Introduction

Under seismic action, reliance for survival of fixed-base structure is placed on its ability to dissipate seismic energy, which occurs while undergoing large inelastic deformations in specially detailed regions of beams and column bases of the gravity load system. With the use of energy dissipation devices (EDDs), which can be easily replaced, it is possible to prevent accumulation of inelastic deformation in the main gravity load resisting members and localization of the damage induced. The basic function of EDDs is to reduce and/or absorb a portion of the input energy, and thereby reducing the energy dissipation demand on primary structural members and minimizing possible structural damage.

A widely considered strategy for the dissipation of energy in the structure during an earthquake is through the inelastic deformation of metallic devices [1–3]. Flexure yielding of steel dampers such as TADAS, ADAS were developed using steel plates of triangular shapes to maximize energy dissipation potential [4–6]. Solid and slit webs of steel section has also shown to yield in shear and act as a damper under lateral loads [7–9]. A few studies have also been carried out on low yielding steel shear panels utilizing its shear deformation as a means to dissipate the energy [10].

The shear yielding of low yielding alloy metals, such as aluminum, has been found to be very ductile and large inelastic deformations are possible without tearing or buckling. The yielding in shear mode maximizes the material participating in plastic deformation without excessive localized strains. In this regard I-shaped shear-links of low yield ductile alloys of Aluminum have been found to be excellent energy dissipative devices limiting the energy dissipation demand on structural members of the primary structure [11–13]. Further, the addition of aluminum shear-links to an ordinary chevron braced frame (OCBF) as shown in Fig. 1 has shown to improve its seismic performance remarkably. The analytical study indicated that addition of shear-links leads to considerable reductions in the base shear which acted as dampers by dissipating significant amount of seismic energy induced in the structure. A number of element tests on the reduced and full-scale shear-links showed satisfactory performance over a wide range of frequencies [11,14]. However, no system test by means of fixing the shear-link within a steel frame has been conducted to verify the effectiveness of shear-link braced frames (SLBFs).

Earthquake simulation tests are an invaluable source of information for understanding the behavior of the structural systems in the nonlinear range. Shaking table tests were conducted to evaluate the load resistance mechanism, failure/damage pattern and the hysteretic behavior of shear-link systems and to provide the data for developing suitable design procedures for proportioning various elements of the overall system.

* Corresponding author.
*E-mail addresses:* dcrai@iitk.ac.in (D.C. Rai), praveen@zentech-usa.com (P.K. Annam), ptripti@iitk.ac.in (T. Pradhan).

0141-0296/$ - see front matter © 2012 Elsevier Ltd. All rights reserved.
http://dx.doi.org/10.1016/j.engstruct.2012.08.027

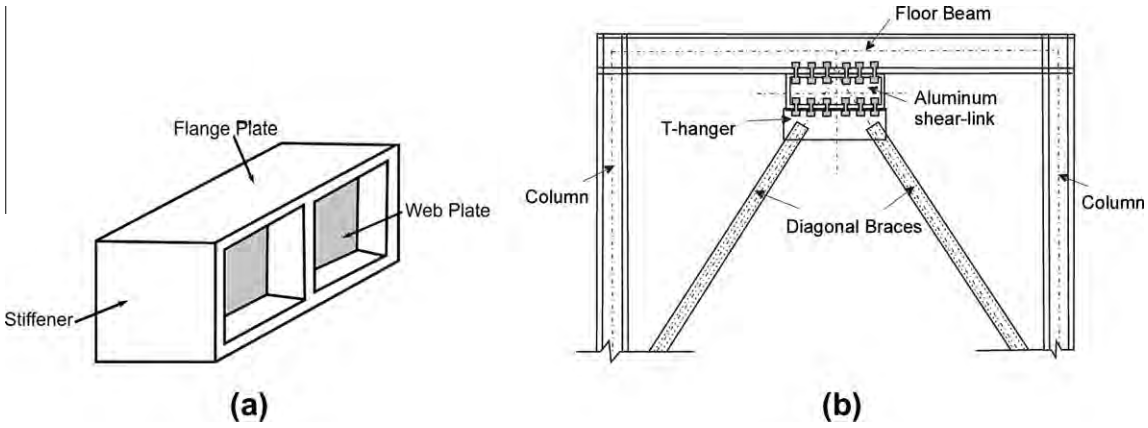


**Fig. 1.** (a) Schematic diagram of typical shear-link and (b) arrangement of shear-link in shear-link brace frame system (SLBF).

The primary objective of this research effort is to study the performance of the SLBF, designed as per the simplified method developed by Rai and Wallace [11], using shake table experiments. A 1:12 reduced scale model was fabricated with due care of dynamic similitude relations and earthquake simulation tests were conducted. The performance of the SLBF was evaluated in terms of floor accelerations, base shears, overturning moments, and hysteretic response of shear-links. Similarly, OCBF model having same details as that of SLBF model was tested in order to compare the performance with the SLBF.

## 2. Aluminum shear link as seismic damper

Typical shear-link with two panels is shown in Fig. 1, which is fabricated from thin plates forming its flanges, web and stiffeners. The aluminum shear-link is designed to yield in shear mode to limit the maximum lateral force, which is transmitted to the primary structure, and to provide significant energy dissipation potential during the earthquake ground shaking by means of inelastic deformation in the damping device. In addition, significant amount of strain hardening of aluminum alloys allows the shear-links to resist additional lateral loads after the first yield and thus forcing shear-links of other stories to share the load in a multi-storied structure. Consequently, the inelastic activities are spread out across various bays and stories of the building structure. These properties make the aluminum shear-link attractive for both new buildings and improvement to existing structures. Aluminum links should be placed strategically in the structure to yield in shear; for example, in ordinary chevron braced frames it is placed in between the diagonal braces and the floor beam as shown in Fig. 1 [11].

## 3. Earthquake simulator testing

### 3.1. Prototype building

A two-storey community building assumed to be located in seismic zone V (PGA = 0.36*g*) on the soil profile Type I (Rock, or hard soil) of IS 1893(Part 1) [15] was considered for analysis. In the plan, the building is 36 m long in the E–W direction (six bays @ 6 m) and 18 m (three bays @ 6 m) wide in the N–S direction as shown in Fig. 2. In the elevation, floor to floor heights are 4.5 m and the building is assumed to possess no irregularity of any kind. In the N–S direction, six bracing frame system were designed to provide the code level lateral resistance. The building was assumed to have a dead load and live load of 3.8 kPa and 3 kPa, respectively, on roof and floor. The six bracing frame systems at the middle bay in N–S direction are designed as SLBF systems and all the other interior frames were designed to resist only gravity loads associated with their tributary areas.

The capacity design approach is followed in proportioning various components of the SLBF system. They are designed for the capacity of the dampers such that the frame does not yield before the dampers reach their failure shear stress. Similar design philosophy has been used for such yielding energy dissipation devices [16,17]. The shear-links are designed based on two limit states of strength and ductility demands of the design level and maximum credible earthquakes. Size of shear link is calculated by determining the horizontal web area required to resist the design storey shear taken same as that of OCBF. The design shear strain, $\gamma_d = \delta/d$ corresponds to the allowable storey drift, $\delta$ at design level earthquake (typically 0.4% of storey height) and the depth $d$, of

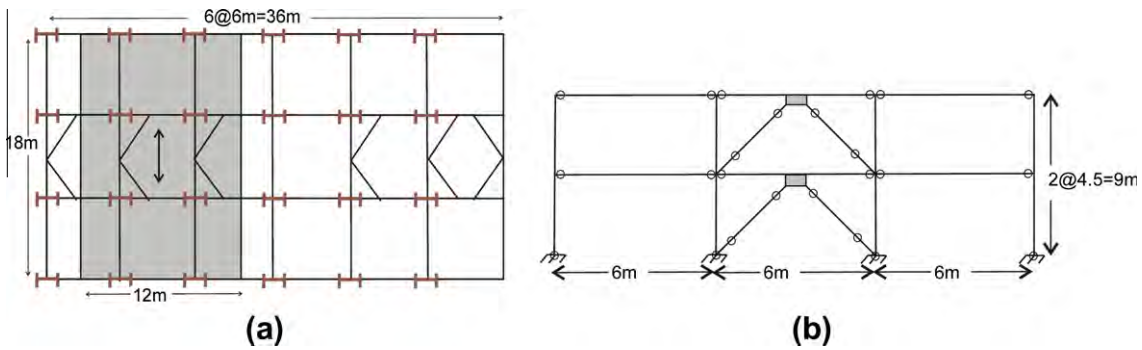


**Fig. 2.** (a) Portion of building and its tributary loading area of the prototype considered for the model and (b) cross-sectional view of the frame under consideration.

**Table 1**
Design calculations.

Zone factor, $Z = 0.36$
Importance factor, $I = 1.5$
Response reduction factor, $R = 4.0$
Fundamental natural period, $T_a = 0.09h\sqrt{d} = 0.19$ s
Average response acceleration coefficient, $S_a/g = 3.5$ (for 5% damping and load factor of 1.4)
Design seismic coefficient, $A_h = \frac{ZI}{2R}\frac{S_a}{g} = 0.236$

Dead load on floors and roof = 3.8 kPa
Live load on floors and roof = 3.0 kPa
Seismic weight on floor and roof = 2948.4 kN
Total seismic weight, $W = 5897$ kN
Design base shear, $V_B = A_h W = 1392$ kN
Design base shear/frame = 1392/6 = 232 kN
Maximum increase due to 5% accidental eccentricity $\frac{V_B(e=1.8)(18)}{2(6^2+12^2+18^2)} = 0.032V_B = 45$ kN

*1. Vertical Distribution of design seismic shears*

| Level | $h$ (m) | $w_x$ (kN) | $w_x h_x^2$ (kNm) | $F_x$ (kN) | $V_x$ (kN) | $V_x^t$(kN) |
|---|---|---|---|---|---|---|
| First | 9.0 | 2948.4 | 238820.4 | 185.6 | 185.6 | 230.6 |
| Ground | 4.5 | 2948.4 | 59705.1 | 46.4 | 232 | 277 |
| $\Sigma$ | | 5897 | 298525.5 | | | |

*2. Proportioning of Shear-link*

| Level | Shear link height (mm) | Allowable storey drift (mm) | Design shear | | Eqiv. AISC section | Shear link dimensions (mm) | | | | | |
|---|---|---|---|---|---|---|---|---|---|---|---|
| | | | Strain $\gamma_d$ | Stress, $_{max}$* (MPa) | | Prototype | | | Model | | |
| | | | | | | $l$ | $d$ | $t_w$ | l | d | $t_w$ |
| First | 375 | 18 | 0.048 | 34.0 | W 14 × 145 | 400 | 375.4 | 17.3 | 42.5 | 28 | 1.17 |
| Ground | 450 | 18 | 0.04 | 32.8 | W 18 × 50 | 956.2 | 456.9 | 9 | 50 | 37.5 | 1.27 |

*3. Design of braces*

| Level | Maximum Shear capacity, $F_{max}$ | Design buckling load, $\frac{F_{max}}{2\cos\theta}$(kN) | Buckling load (kN) | Brace section | |
|---|---|---|---|---|---|
| | | | | Prototype | Model |
| First | 306.3 | 257.6 | 249 | ISHB 150@34.6 kg | 7 mm dia, 1.5 mm thick |
| Ground | 381.7 | 321 | 437 | ISHB 200@37.3 kg | 10 mm dia., 1.6 mm thick |

* $\tau_{max} = 2.6\sigma_{0.2}\gamma^{0.2}$, $\sigma_{0.2} = 24.01$ MPa, $\theta = 53.5$ °.

**Table 2**
Scale ratios for dynamic similitude adopted for modeling.

| Parameters | | Scale ratio |
|---|---|---|
| Length | $S_l$ | 1/12 |
| Modulus | $S_E$ | 1 |
| Acceleration | $S_a$ | 2 |
| Time scale | $S_T = \sqrt{\frac{S_l}{S_a}}$ | $\sqrt{\frac{1}{24}}$ |
| Mass | $S_M = \frac{S_E S_l^2}{S_a}$ | 1/288 |
| Strain | $S_\varepsilon$ | 1 |
| Stress | $S_\sigma$ | 1 |

shear-link is chosen between 1/10th and 1/12th of storey height. The peak shear stress and strain values in the shear-links follow a power law relation given by $\tau_{max} = 2.6\ \sigma_{0.2}\gamma^{0.2}$ where $\sigma^{0.2}$ is the tensile yield strength of web material [11].

The maximum allowable shear strain is assumed to be 20% and strains higher than this value represents failure of shear links. The braces are proportioned such that their buckling load is greater than the axial force corresponding to shear stress in the link at 20% shear strain, which is taken as 1.886 times $\sigma^{0.2}$, the tensile yield strength of web material. The design calculations for shear links and braces are summarized in Table 1.

### 3.2. Model

The experimental model represents a portion of the building which corresponds to two sets of isolated braced frames (SLBF or OCBF) designed to resist inertial forces developed due to loads on corresponding tributary areas, as shown in Fig. 2. The assumption is justifiable considering that the excitation is only in one direction. For a reliable correlation with the prototype, it is important that the modeling is appropriate with respect to governing similitude relations [18]. Based on the size and capacity of the shake table an optimum length-scaling ratio of 1:12 was adopted. An acceleration ratio of 2 was adopted to reduce the required mass for limited space available in the model. For adequate dynamic simulation, acceleration, time and frequency scale ratios were modified according to applicable similitude relations, as shown in Table 2. The similarity in buckling behavior is valid for shear-link models, even in the inelastic range, as strain number is same for both model and prototype [19].

Tubes sections were used for frame members because of ease in fabrication. The dimensions of the shear link required were computed from the formulation developed by Rai and Wallace [11] and results are summarized in Table 1. Braces were proportioned such that they do not buckle before the shear stress in the links reached the failure shear stress. Pipe sections were chosen for braces because the fracture life and ductility are greater than those of rectangular tube sections. In this present study, the braces and other members of the OCBF were kept the same, as in the SLBF, to facilitate a direct comparison. All the beam and columns were cut to the required lengths from the corresponding tube sections, and pinned connected at the ends. Floor beams were connected to the column through two bracket plates welded on both sides of the column. The beam was connected to the plates through a pin to simulate a hinged end connection and a gap of 5 mm was left from the edge of the beam to the column for free rotation of the pin joint during loading. All the columns were connected to base beam through pin connection. The schematic diagram of the model is illustrated in Fig. 3 and details of various connections are shown in Fig. 4.

The energy dissipation capacity of the shear panels depends strongly on the mechanical properties of the material. A highly ductile material is needed to meet the large inelastic strain demand required in these applications. In this investigation, specimens were fabricated from commonly used alloy of aluminum 1100-O. These

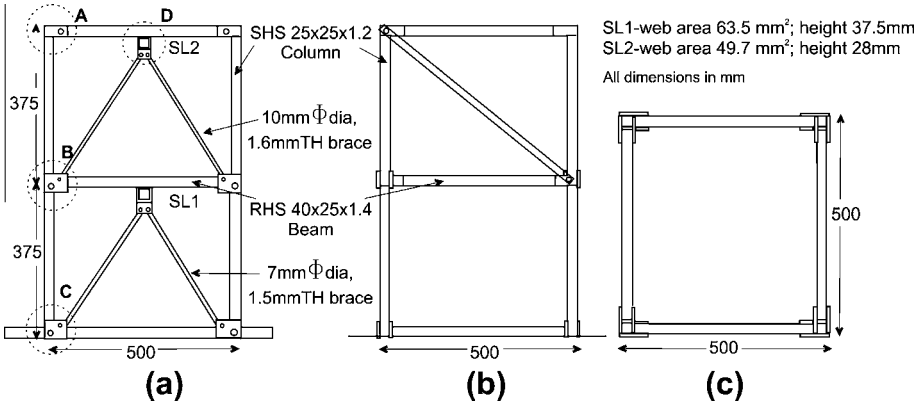


**Fig. 3.** Model specimen frame and its members: (a) Front elevation, (b) side elevation, and (c) plan.

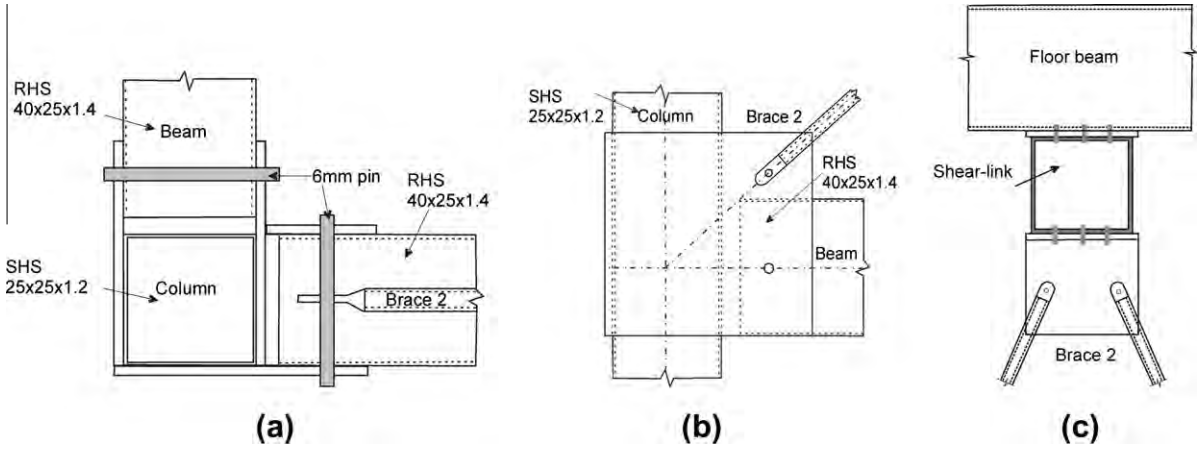


**Fig. 4.** Details of (a) plan of connection A, (b) elevation of connection B, and (c) elevation of connection D.

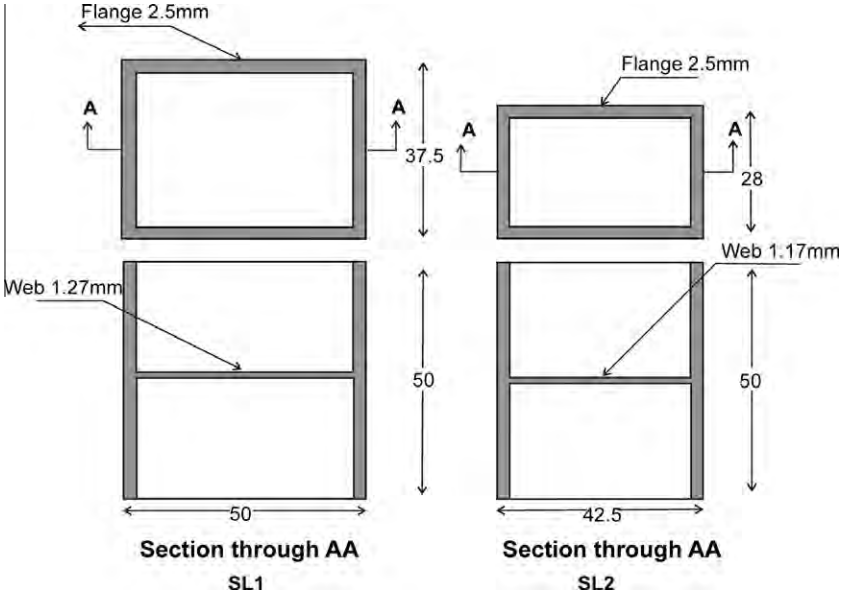


**Fig. 5.** Dimensions of the fabricated shear-link used in the experiment.

were machined from a larger piece because of greater accuracy needed for very thin web (1.11–1.28 mm). The details of the fabricated shear-links are shown in Fig. 5. To relieve the initial stresses and stresses developed close to the surface during machining, the shear-links were heat treated (annealed). They were raised to a temperature of 420 °C for two hours and then gradually cooled at a rate of 30 °C per hour in heat treating oven. The mechanical properties of the material used in the test specimens were obtained from

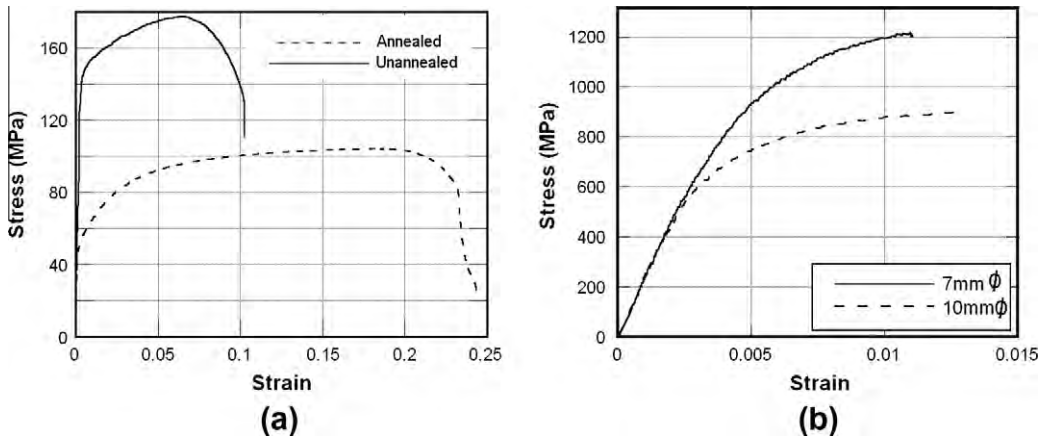


**Fig. 6.** Tensile stress–strain curve for (a) aluminum alloy used and (b) steel brace used in the model.

uni-axial tension tests on un-annealed and annealed coupons. The coupons were made from the strips that were cut out of the solid square section. The 0.2% proof stress for unannealed 1100-O was about 150 MPa while after annealing the yield stress reduced to 53.6 MPa, as shown in Fig. 6a. The stress–strain curves for the tubular steel braces of 10 mm and 7 mm dia. used in the model are shown in Fig. 6b. The corresponding 0.2% proof stress are 820 MPa and 1040 MPa, respectively.

### 3.3. Test set-up

The uni-axial shake table used for testing had the dimensions of 1.8 m × 1.2 m (length × width) with 1.8 m length in the direction of motion [20]. The test specimens were instrumented with accelerometers, displacement transducers and strain gages to measure the required response. Two accelerometers, one at each floor level were placed to measure the floor's absolute accelerations. Similarly, table acceleration was measured using the accelerometer attached to it. Displacement transducers (LVDTs) were used to measure floor displacements. At the mid-length of each column and brace, strain gages were used to measure axial force. A sampling period of 0.0026 s (393 Hz) was adopted for acquisition of data through a high performance data acquisition system. Fig. 7a and b represents specimen mounted on the shake table.

### 3.4. Loading history and earthquake simulation

A series of earthquake simulation tests were performed by using the uniaxial shaking table. The target accelerogram of the table was the recorded component of the 1952 Taft earthquake (Taft N21E with PGA of 0.15g). A comparison of acceleration response spectrum of Taft ground motion is performed with response spectrum used for the design of the prototype and model as per IS 1893 [15]. The scaled Taft motion with PGA equal to 0.2g matched reasonably well with the code spectrum in highest seismic zone as shown in Fig. 8 and it can be considered to represent the 'intensity' or 'severity' implied by the design-basis earthquake (DBE). As a result, the test run TAFT04 was chosen to represent the DBE level ground motion for the prototype and model and others test runs were expressed as percentage of DBE, for example, TAFT08 can be referred as 200% DBE. The 150% DBE was regarded as the code level design earthquake with importance factor of 1.5 used for structures with higher consequences of failure, such as hospitals, schools, and community buildings. Similarly, 200% DBE was considered to represent maximum credible earthquake (MCE), whereas the 400% DBE can be thought to represent a 'catastrophic' level earthquake. The prototype and model structure were designed for 150% DBE as the actual design earthquake load for the study building which was intended to serve as community building. It should be noted that the 100%DBE does not include the importance factor of 1.5 considered for the study building.

Based on the similitude rules the time axis was compressed by a scale factor of $\sqrt{\frac{1}{24}}$ (Table 2). The original Taft ground motion, scaled motion and their response spectra are shown in Fig. 8. For several runs of time scaled Taft motion, only PGA was varied in increments of 0.1g, starting with 0.1g and carried up to the failure of specimen. White noise tests (with PGA of 0.05g) were conducted


**Fig. 7.** (a) Specimen mounted over the shake table and (b) close up view of shear link.

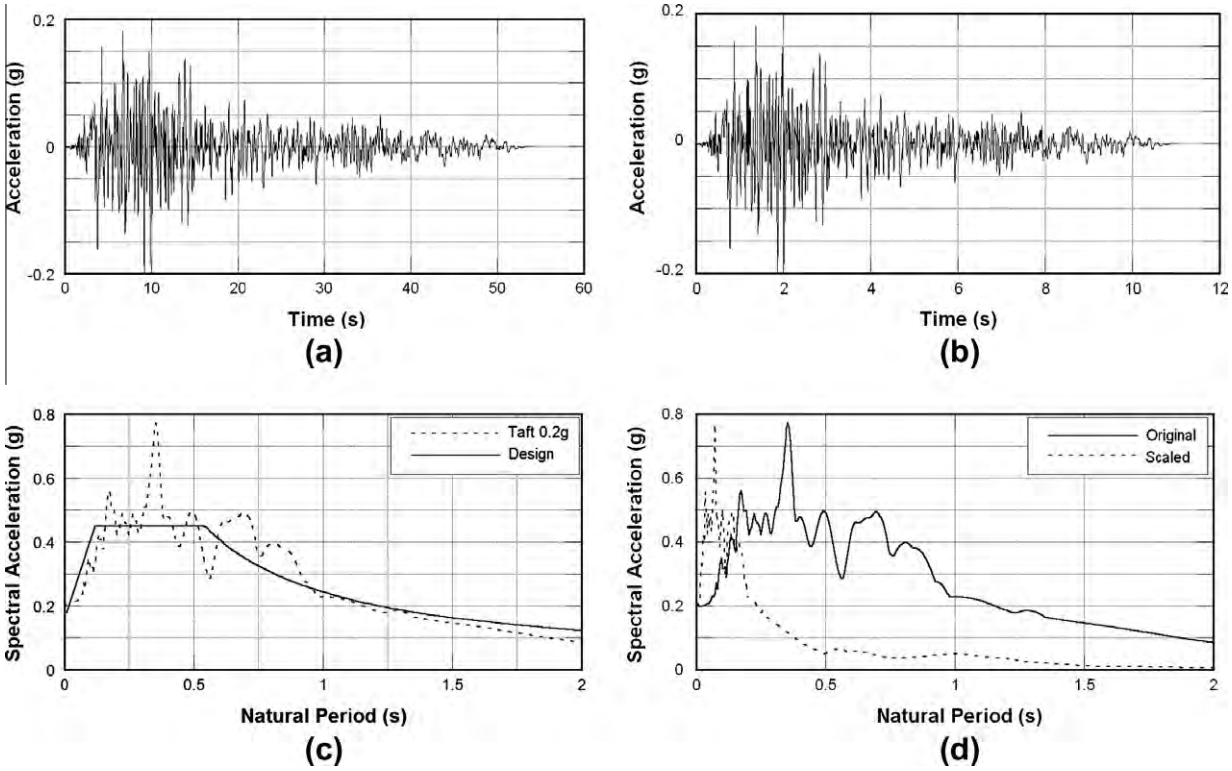


**Fig. 8.** (a) Original Taft N21E component of 1952 Taft earthquake, (b) scaled motion, (c) comparison of design response spectra and Taft 0.2*g* response spectrum, and (d) response spectra comparison of the original and scaled ground motion.

**Table 3**
Fundamental frequency measurements.

| Test | Natural frequency (Hz) | |
|---|---|---|
| | SLBF | OCBF |
| Ambient vibration test | 7.4 | 9.6 |
| Free vibration test | 7.0 | 9.7 |
| Forced vibration test | 7.3 | 9.8 |

after each earthquake simulation test to investigate the change in the stiffness properties of the model.

## 4. Dynamic characteristics

### *4.1. Free vibration test*

Free vibration is the natural response of a structure to some initial displacement or velocity. The response is completely determined by the properties of the structure. An impact hammer and a medium tip along with extender mass were used. The signal from the quartz force sensor was acquired and its Fourier transform showed the force spectrum to be flat over a wide range and, therefore could excite the modes present in this range. The response was measured with the help of two velocimeters, one at each floor. The hammer was struck at different locations of the model and on the table, and floor velocity time histories were obtained at a sampling frequency of 1000 Hz, a signal conditioner was used to amplify the signal and to filter out the noise. Natural frequencies of the SLBF and OCBF models are summarized in Table 3.

### *4.2. Forced vibration test*

Generally forced vibration test are conducted where the ambient noise is not sufficient to obtain the response of the system. An electro-dynamic shaker was used as an excitation source. Forced sinusoidal vibration test was performed at different frequencies. The first sweep of tests indicated some narrow range of frequencies in which the model's natural frequency could be expected. The frequency content of the time history was evaluated and the peak amplitudes were plotted against the corresponding exciting frequencies, and the frequencies corresponding to maximum peak amplitudes were regarded as natural frequencies.

## 5. Evaluation of earthquake test results

### *5.1. Overall behavior and failure mechanism*

The response of a system to dynamic excitation depends on properties, such as natural periods and modes of vibration, damping; and yield strength and hysteretic characteristics in case of inelastic systems. For earthquake excitation below 100% DBE (i.e., model PGA of 0.4*g*), no inelastic activity or damage was noticed for both OCBF and SLBF. However, at 125% DBE, elastic buckling of first floor braces in OCBF was observed along with a premature failure of pin connection. The pin was replaced and further tests were continued. The permanent bending of second floor braces of OCBF occurred at 200% DBE. During the test run corresponding to model PGA of 1.1*g* (i.e., 275% DBE), the second storey brace fractured which seriously undermined the lateral load capacity of OCBF and further test runs were not carried out.

In contrast, for the same level of excitation (275% DBE), only inelastic activity in SLBF was the buckling of the first floor shear-links, whereas all other members were in the elastic region. The buckling of second floor shear-links was noticed at 375% DBE. The SLBF continued to sustain even higher levels of excitation and when the test was stopped at 425% DBE, severe buckling had taken place in shear-links of both stories. However, no other

**Table 4**
Summary of observations.

| Test run ID | PGA (g) | | % DBE | Observations | |
|---|---|---|---|---|---|
| | Model | Prototype | | SLBF | OCBF |
| TAFT02 | 0.2 | 0.10 | 50 | – | – |
| TAFT04 | 0.4 | 0.20 | 100 | No inelastic damage or activity | No inelastic damage or activity |
| TAFT05 | 0.5 | 0.25 | 125 | – | Buckling of first storey braces, connecting pin failed and replaced after |
| TAFT08 | 0.8 | 0.4 | 200 | First storey shear-link suffered significant plastic shear distortion. Rosettes detached due to higher shear strains | Permanent bending in second storey braces identified |
| TAFT11 | 1.1 | 0.55 | 275 | Web buckling of first storey shear-links observed | Second storey braced fractured which seriously undermined the lateral load capacity. Tension failure of first floor brace at connection noticed |
| TAFT15 | 1.5 | 0.75 | 375 | Web buckling of second storey shear-links | – |
| TAFT17 | 1.7 | 0.85 | 425 | Severe buckling of shear-links of both storey | – |

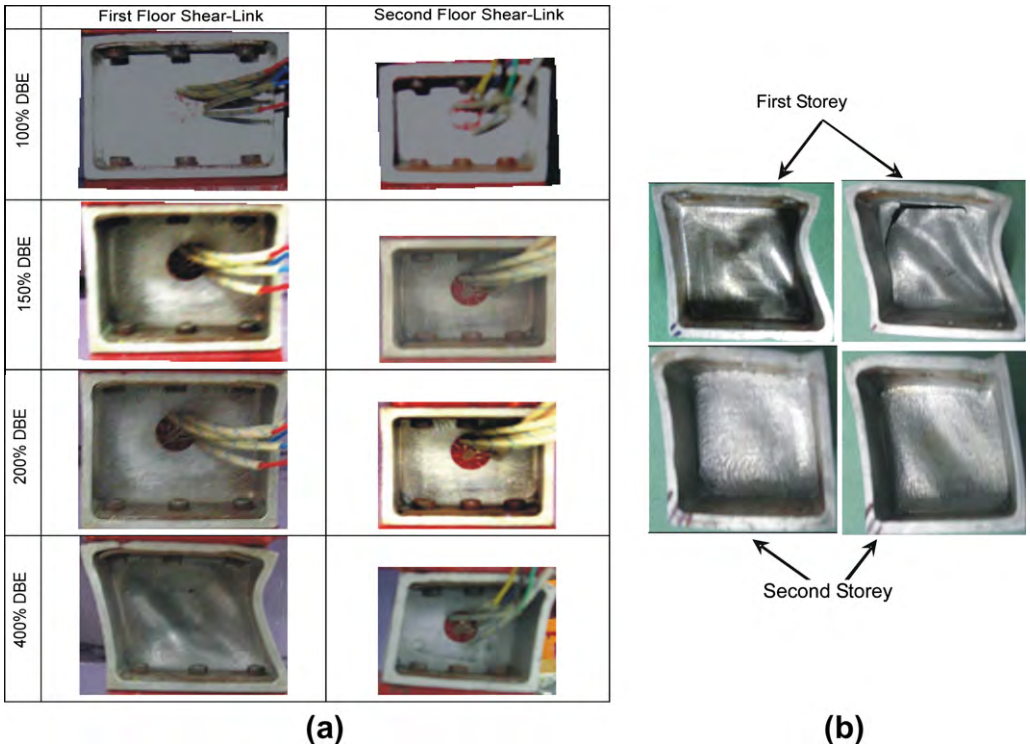


**Fig. 9.** (a) Deformed configurations of shear-links at different level of excitation and (b) deformed shear-links after the TAFT17 Test (425% DBE).

member of the frame had experienced any inelastic deformation or damage. The primary events related to deformation and damage of the modes at various levels of earthquake excitation are summarized in Table 4. The buckled shear-links after the last test run TAFT17 corresponding to model PGA of 1.7*g* are shown in Fig. 9. At the end of the test, no tearing of the web was observed, though very deep buckles (folds) were present in the web. Web tearing in one of the first floor shear-link occurred suddenly when it was being removed from the frame, possibly due to readjustment of internal stresses at the release of restraint.

Fig. 9 shows the deformed configuration of shear-links at various levels of excitation. As discussed above, until 200% DBE, the first storey links suffered significant plastic shear distortion, while the second storey links 'nearly' maintained the original geometry. Significant yielding and buckling of web, flanges and end stiffeners was noticed at the excitation level of 400% DBE. Despite such visible distress, the links maintained their own structural integrity and that of the SLBF, at such a high intensity of shaking. Since the shear-links were not replaced after each run, the yielded and buckled shear-link softened the entire structure causing increase in the natural period and corresponding reduction in the force demands.

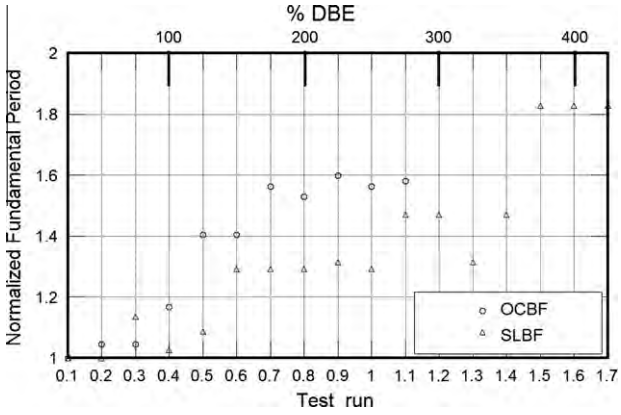


**Fig. 10.** Comparison of white noise fundamental period for OCBF and SLBF.

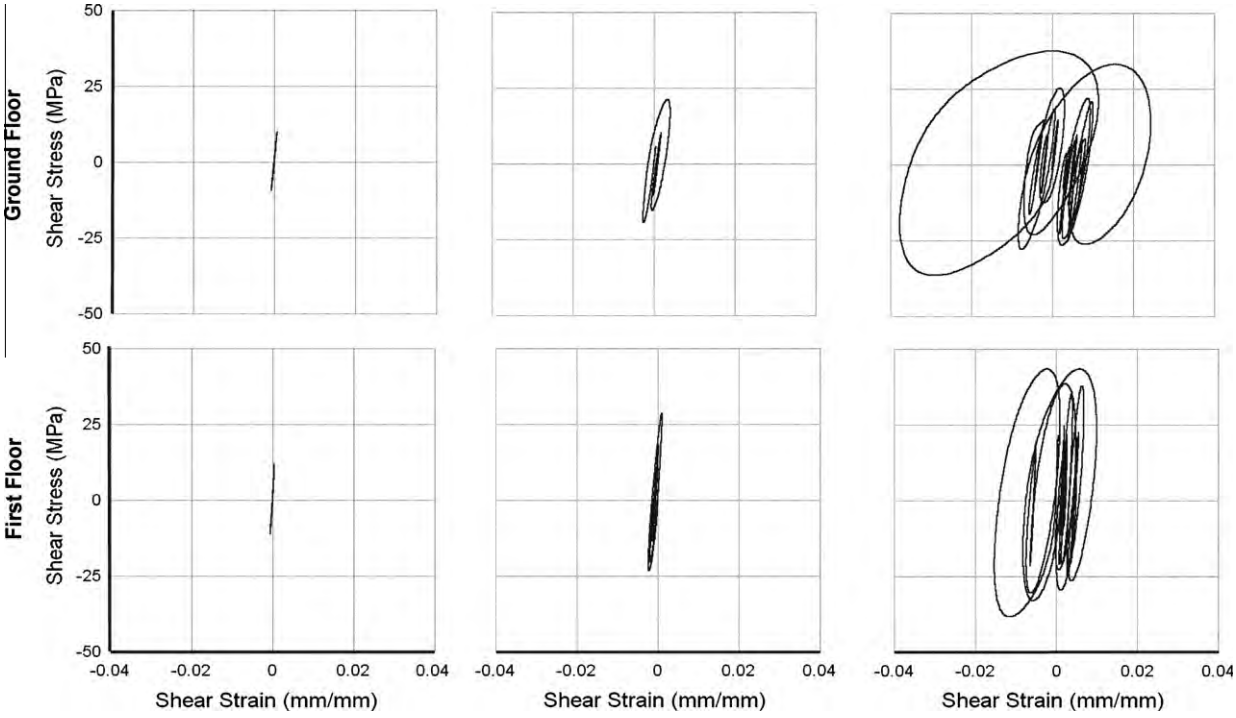


**Fig. 11.** Hysteresis response of shear-links at 50%, 100% and 200% DBE.

The fundamental period of OCBF and SLBF systems for white noise test runs are presented in Fig. 10. The normalized fundamental period shows that there was 80% increase in the period from the first run of 25% DBE to 425% DBE for the SLBF system which increased in steps following the major inelastic events. However, the corresponding decrease in acceleration demand is about 50% which is lower than the total increase in the PGA levels during successive simulations. It should be noted that decrease in floor accelerations is result of the combined effect of decrease in effective stiffness (causing period elongation) and hysteretic characteristics of the yielding components (causing increase in 'damping').

Shear stress in shear links was obtained from the horizontal component of brace forces divided by link web area, whereas shear strains were directly measured using strain rosette in the web which are seen as dark circle in Fig. 9a. At 100% DBE, shear-links experienced very little or no inelastic deformations, which increased only marginally at 150% DBE. Shear-links in the first-storey experience larger shear stress in comparison to second storey links. Further, even at 200% DBE, the maximum shear strain was about 4% in first storey and about 2% in the upper storey. Throughout all test runs, shear links at different floors have shown the stable hysteresis loops. (Refer Fig. 11.)

### 5.2. Acceleration response

The floor acceleration time-histories for OCBF and SLBF at 50, 100 and 200% DBE are plotted in Fig. 12. These plots show that the SLBF system was effective in reducing the peak acceleration of both the floors compared to the OCBF system for the same level of excitation. Peak accelerations at different floors of SLBF system are substantially smaller than those observed for OCBF system for all acceleration levels as shown in Fig. 13. In other words, the inertial forces developed at different floors, which needed to be resisted by the bracing system were smaller in SLBF system in comparison to OCBF system. The peak floor accelerations of the SLBF system increased at progressively decreasing rate. The SLBF system had shown better performance in reducing the peak floor accelerations during the tests of higher PGA values.

### 5.3. Base shear and overturning moments

Base shears indicate the global seismic demand imposed on the model structure for various excitation levels of the Taft ground motion. These were determined from the first storey brace forces, which were derived from axial strains measured using strain gages. Similarly, base overturning moments (OTMs) were derived from the column axial forces measured from axial strains in the first storey columns. As noted in the case of floor acceleration response, the general characteristics of force quantities, base shear and OTMs do not change significantly with increase in earthquake excitation level. Further, the nature of time-histories of base shear and OTMs are nearly similar, indicating that columns primarily resisted OTMs, while the lateral shear was almost entirely resisted by the braces and/or shear-links.

The SLBF system attracted lower base shear than OCBF during all simulation tests and the reduction ranged from about 41–64%. Moreover, it can be observed in Fig. 14a that the SLBF system attracted base shear at a progressively decreasing rate. This can be attributed to the fact that the further yielding of shear links at both floor levels made the SLBF system more flexible indicated by increase in natural periods (Fig. 10), and larger energy dissipation (damping) by shear-links due to higher drifts (strains) at increased PGA levels of loading. Consequently, SLBF attracted base shear at much decreased rate and was limited by the post-yield/buckling capacity of shear-links which was kept reasonably low.

Similarly, the SLBF system was subjected to lesser overturning moments than the OCBF system. Reduced maximum base overturning moments resulted in lesser peak forces in the primary members. It is clear from these observations that SLBF system is capable of limiting the forces transferred to the primary structural members, at all levels of ground motion. As in the case of base

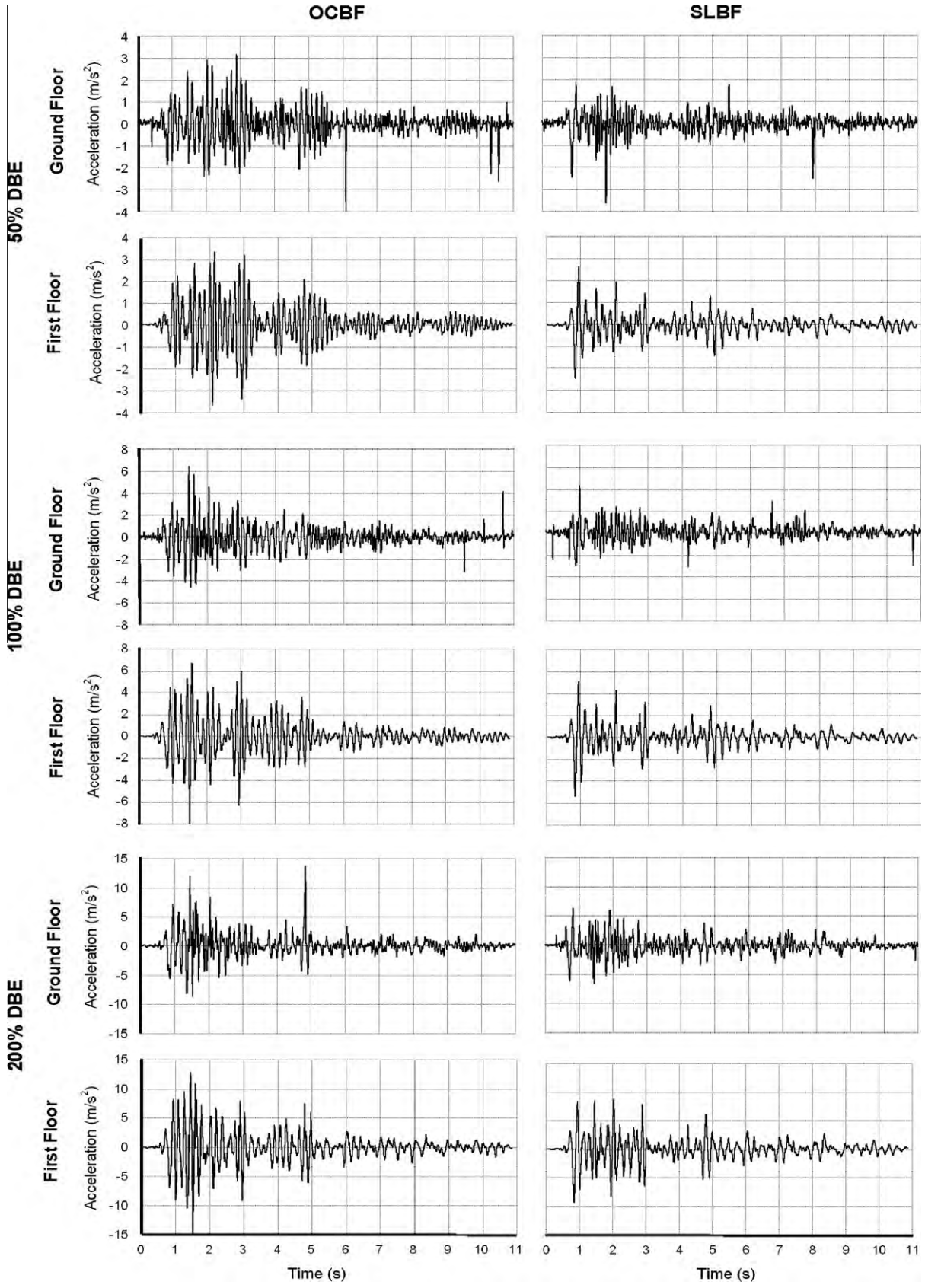


**Fig. 12.** Time history analysis of ground floor and first floor acceleration of OCBF and SLBF at 50%, 100% and 200% of DBE.

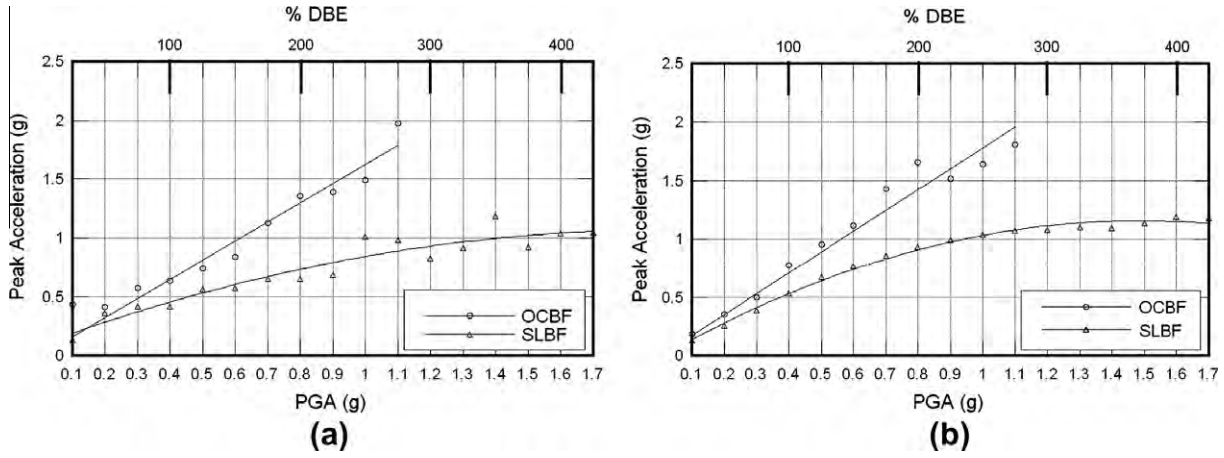


**Fig. 13.** Comparison of peak accelerations of OCBF and SLBF (a) first floor and (b) second floor.

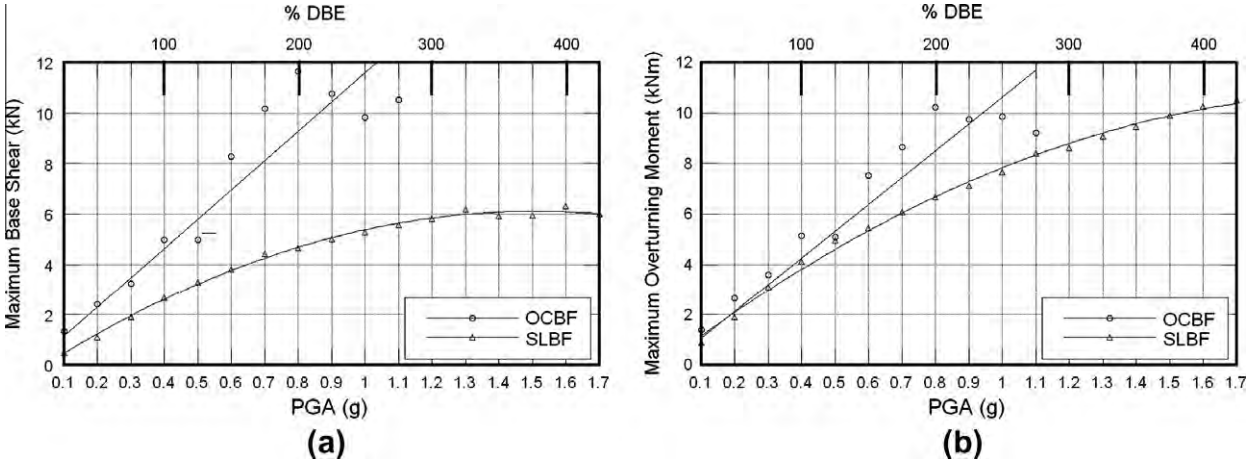


**Fig. 14.** (a) Comparison of maximum base shears of OCBF and SLBF, and (b) comparison of maximum base overturning moments of OCBF and SLBF.

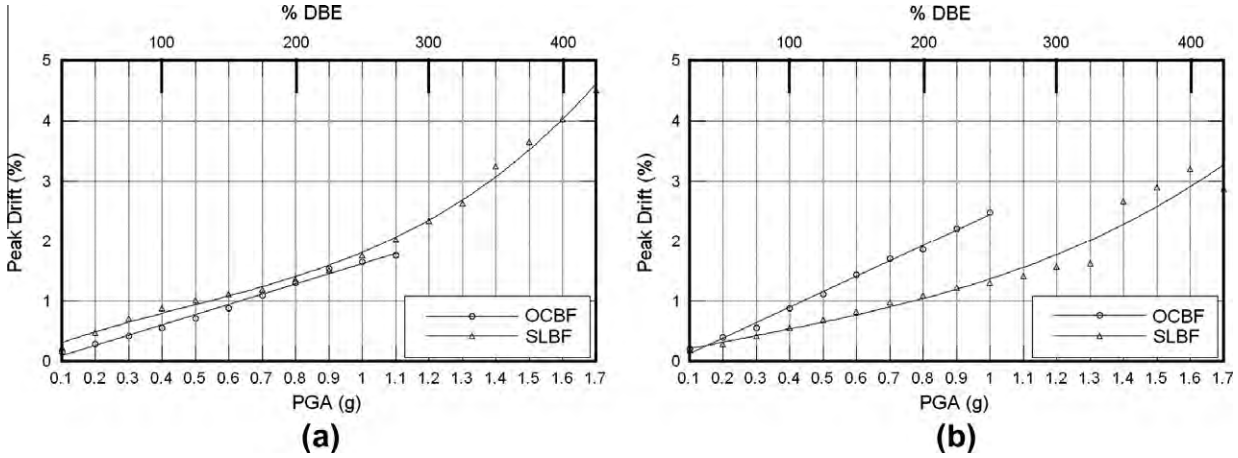


**Fig. 15.** Comparison of peak drifts of OCBF and SLBF (a) first floor and (b) second floor.

shear, the overturning moment also increased at a progressively decreasing rate with increasing severity of ground motion as shown in Fig. 14b. These results clearly indicate the effectiveness of shear-links in limiting the seismic demand on the structure as a whole and in the primary structural member such as columns and braces.

### 5.4. Floor drifts

The first floor storey drifts of SLBF were always greater than the OCBF system for all test runs, whereas the second storey drifts of SLBF were smaller than those of OCBF (Fig. 15). Further, the increased storey drifts were not so large to cause extensive non-structural damages; they were about 1% at 150% DBE, which increased to about 1.3% for 200% DBE excitation. The SLBF system had increased floor displacements in comparison to OCBF by a factor of 1.03–1.14. However, care must be taken for SLBF in tall structures as they tend to be more sensitive to additional P-delta effects.

## 6. Summary and conclusions

Reduced scale models (1:12) of ordinary concentric braced frame (OCBF) and frame supplemented with aluminum shear link (SLBF) were subjected to a series of scaled Taft ground motion with increasing severity, and the results were evaluated and compared:

The SLBF system attracted less base shear during simulation tests compared to OCBF. Peak base shears were observed to be progressively decreasing with increasing severity of ground motion with maximum reduction to about 64%. Due to yielding and/or buckling of shear-links at lower lateral loads, the shift in natural periods due to reduced effective frame stiffness and enhanced energy dissipation due to hysteresis helped in decreasing the acceleration demand at higher PGA levels of successive simulations. Similarly, overturning moments and floor accelerations were substantially smaller in SLBF than those observed for the OCBF system. With decrease in frequency, there has been corresponding increase in drift levels which may be critical for tall structures. In SLBF, all inelastic activities were confined to shear-links as expected, while the other structural members remained in the elastic range even up to 1.7*g* PGA (425% DBE) of simulated motions. In comparison, braces of OCBF buckled permanently and deformed at much lower PGA of 1.1*g* (275% DBE).

The scaled model specimens captured the overall behavior rather accurately. Various response quantities for the corresponding prototype structure can be obtained by employing the same scaling factors used for geometry and loading for these scaled models within the margin of errors of modeling and experimentation. However, these results needs to be further investigated analytically or preferably conducting tests on large scale specimens to preclude errors due to variations in geometry, dimensions and connection details which are rather difficult to control in small-scaled models.

## Acknowledgments

The financial support provided by the Ministry of Human Resource Development, and Council of Scientific and Industrial Research, Government of India, New Delhi in carrying out this experimental research work is gratefully acknowledged. The authors greatly appreciate the quality work of Mr. Digambar Urukude of the Structures Lab, Indian Institute of Technology Kanpur in constructing the test apparatus and help from Mr Vaibhav Singhal, PhD scholar, in reviewing the experimental data.

## References

[1] Soong TT, Dargush GF. Passive energy dissipation systems in structural engineering. New York: John Wiley & Sons; 1997.
[2] Soong TT, Spencer Jr BF. Supplemental energy dissipation: state-of-the-art and state-of-the-practice. Eng Struct 2002;24(3):243–59.
[3] Sahoo DR, Rai DC. Seismic strengthening of non-ductile reinforced concrete frames using aluminum shear links as energy-dissipation devices. Eng Struct 2010;32(11):3548–57.
[4] Whittaker AS, Bertero VV, Thomson CL, Alonso LJ. Seismic testing of steel plate energy dissipation devices. Earthquake Spectra 1991;7(4):563–604.
[5] Tsai K, Chen H, Hong C, Su Y. Design of steel plate energy absorbers for seismic-resistant construction. Earthquake Spectra 1993;9(3):505–28.
[6] Bergman DM, Goel SC. Evaluation of cyclic testing of steel plate devices for added damping and stiffness. Report no. UMCE87-10. Ann Arbor (MI, USA): The University of Michigan; 1987.
[7] Chan RWK, Albermani F, Williams MS. Evaluation of yielding shear panel device for passive energy dissipation. J Construct Steel Res 2009;65:260–8.
[8] Zhengying L, Albermani F, Chan RWK, Kitipornchai S. Pinching hysteretic response of yielding shear panel device. Eng Struct 2011;33(3):993–1000.
[9] Chan RWK, Albermani F. Experimental study of steel slit damper for passive energy dissipation. Eng Struct 2008;30:1058–66.
[10] Nakashima M, Iwai S, Iwata M, Takeuchi T, Konomi S, Akazawa T, Saburi K. Energy dissipation behaviour of shear panels made of low yield steel. J Earthquake Eng Struct Dynam 1994;23:1299–313.
[11] Rai DC, Wallace BJ. Aluminum shear link for enhanced seismic resistance. J Earthquake Eng Struct Dynam 1998;27:315–42.
[12] Matteis GD, Mazzolani FM, Panico S. Pure aluminum shear panels as dissipative devices in moment resisting steel frames. J Earthquake Eng Struct Dynam 2007;36(7):841–59.
[13] Sahoo DR, Rai DC. A novel technique seismic strengthening of RC frame using steel caging and aluminum shear yielding device. Earthquake Spectra 2009;25(2):415–37.
[14] Jain S, Rai DC, Sahoo DR. Post yield cyclic buckling criteria for aluminum shear panels. J Appl Mech 2008;75(2):1015-1–8.
[15] BIS. IS:1893 Indian standard criteria for earthquake resistant design of structures, part 1: general provisions and buildings, Fifth revision. New Delhi: Bureau of Indian Standards; 2002.
[16] Karavasilis TL, Kerawala S, Hale E. Hysteretic model for steel energy dissipation devices and evaluation of a minimal-damage seismic design approach for steel buildings. J Construct Steel Res 2012;70:358–67.
[17] Lin YY, Tsai MH, Hwang JS, Chang KC. Direct displacement-based design for building with passive energy dissipation systems. Eng Struct 2003;25(1):25–37.
[18] Mills RS, Krawinkler H, Gere JM. Model tests on earthquake simulators development and implementation of experimental procedures, Report No. 39. Stanford University, CA: The John A. Blume Earthquake Engineering Center; 1979.
[19] Singer J, Arbocz J, Weller T. Buckling experiments: experimental methods in buckling of thin-walled structures: basic concepts, columns, beams and plates, vol. 1. John Wiley & Sons, Inc.; 1998.
[20] Sinha P, Rai DC. Development and performance of single-axis shake table for earthquake simulation. Current Sci 2009;96(12):1611–20.